tional Animal Care and Use Committee at Kyoto University and conformed to the Guide for the Care and Use of Laboratory Animals published by the US National Institutes of Health (NIH Publication No. 85–23, revised 1996). The initial surgery to induce hindlimb ischemia has been described previously[12] Briefly, the rabbits were anesthetized with sodium pentobarbital (40 mg/kg, im). Under sterile surgical conditions, a longitudinal incision was made in the medial thigh of one hindlimb, extending from the inguinal ligament to a point just proximal to the patella, to expose and isolate the external iliac artery, which was ligated twice and sectioned between the ligatures. The femoral artery was completely excised from its proximal origin to the point where it bifurcates into the saphenous and popliteal arteries. Blood flow to the hindlimb after excision of the femoral artery is dependent upon flow through the internal iliac artery. The incision was closed in 3 layers with 3.0 nylon filament. All rabbits were closely monitored by veterinary staff and received an antibiotic (cefazolin, 20 mg/kg, s.c.) for 3 days following surgery.

Preparation of Gelatin Hydrogel Microspheres Incorporating bFGF

Gelatin hydrogel microspheres incorporating bFGF were prepared as follows. Gelatin with an isoelectric point (IEP) of 4.9 was isolated from bovine bone collagen by an alkaline process using $Ca(OH)_2$ (Nitta Gelatin, Osaka, Japan). Gelatin microspheres were prepared through glutaraldehyde cross-linking of gelatin in aqueous solution dispersed in an oil phase. A mixture of the gelatin aqueous solution (10 wt%, 0.2 ml) and olive oil (5 ml) was preheated to 40°C, followed by agitation for 1 min. The emulsion prepared was cooled down in crushed ice to allow the formation of natural gelatin for the gelatin aqueous solution. Acetone was then added to the emulsion and stirring was continued for 1 h at 4°C. The resulting microspheres were washed 3 times with acetone (4°C) and recovered by centrifugation at 4,500 g and 4°C for 5 min. The non-cross-linked gelatin microspheres (20 mg) were placed in 20 ml of 0.1 wt% Tween-80 aqueous solution containing 0.13 wt% of glutaraldehyde, and stirred at 4°C for 24 h to facilitate cross-linking. Following collection by centrifugation (4,500 g, 4°C, 5 min), the microspheres were agitated in 20 ml of 10 mmol/L aqueous glycine solution at 37°C for 1 h to block the residual aldehyde groups on unreacted glutaraldehyde. The resulting microspheres were finally washed 3 times with double-distilled water by centrifugation and freeze-dried. The microsphere diameter was measured for at least 100 microspheres under a light microscope to calculate their volume. The average diameter of the microspheres was 10 μm.

Human recombinant bFGF with an IEP of 9.6 was supplied by Kaken Pharmaceutical, Tokyo, Japan and incorporated into the gelatin microspheres by dropping 5 mg/ml of bFGF solution (20 μl) onto 2 mg of freeze-dried gelatin microspheres, which were then left at room temperature for 1 h. The solution (20 μl) was completely absorbed into the microspheres during swelling, because the solution volume was less than that theoretically required for the equilibrated swelling of microspheres.

Experimental Groups

Two weeks after surgery, the rabbits were randomly assigned to 1 of 4 experimental groups (n=11, each group) and treated for 4 weeks: group A, no treatment; group B, supplemented with diet containing sarpogrelate (100 mg/kg per day); group C, single intramuscular injection of sustained-release form of bFGF microspheres (50 μg); group D: combined treatment with sustained-release bFGF and sarpogrelate.

Measurement of Hindlimb Blood Flow

With the use of non-radioactive colored microspheres (diameter, 15.5±0.2 μm; Dye-trak, Triton Technology Ltd, Notts, UK), the resting regional hindlimb blood flow was determined in 5 rabbits from each experimental group[17] Six weeks after surgery, the reanesthetized rabbits were placed in the supine position on a temperature-controlled heating pad. Colored microspheres (3×10^6 particles) were injected into the left ventricle immediately before angiography. Reference arterial blood samples were collected through the aortic catheter, starting 10 s before the injection of the microspheres and continuing for 120 s at the rate of 2 ml/min. Two or more tissue specimens were obtained from the adductor muscle and the gastrocnemius muscle at the time of death. Samples were then placed into Teflon-sealed 16-ml screw-cap tubes and 7 ml of a 4 molar KOH solution containing 2% Tween 80 was added to each sample for digestion of the tissue. The photometric absorption of the resulting samples was measured using a diode array spectrophotometer (UV-1200, Shimadzu, Kyoto, Japan). The number of microspheres in each sample was calculated according to the optical density at the wavelength corresponding to dye color using standardization curves generated from known quantities of microspheres from the sample batch of spheres. Regional blood flow was then determined and expressed as ml/min per 100 g tissue.

Microangiographic Assessment

Six weeks after surgery, 6 rabbits from each experimental group were reanesthetized, and angiographic assessment was performed with synchrotron radiation microangiography with a spatial resolution of 30 μm[18] Contrast material containing 37% nonionic iodine (Iopamidol, Nihon Shering Co, Ltd, Osaka, Japan) was injected using an automated injector (Autoenhance A30–200, Nemoto Kyourindo Co, Ltd, Tokyo, Japan) at a rate of 1.25 ml/s via a 4F catheter placed immediately above the aortic bifurcation. Quantitative angiographic analysis of collateral vessel visualization was performed using a composite of 5×5 mm grids. The angiographic score was calculated as the ratio of grid intersections crossed by opacified arteries divided by the total number of grid intersections in the medial thigh region[19] This analysis was performed by a single observer who was unaware of the treatment regimen.

Histological Determination of Capillary Density

Immediately after the completion of the microangiographic study, the 24 rabbits were killed with an intravenous overdose of pentobarbital and potassium chloride. The hindlimbs were dissected and samples of the adductor muscle were removed for histological evaluation. After the samples were fixed in 10% formalin, followed by embedding in paraffin, they were frozen in liquid nitrogen for immunohistochemistry. The staining of endothelial cells was performed using a monoclonal antibody against CD31 (Dako Cytomation Co, Ltd, Glostrup, Denmark). Five fields from 6 different sections were randomly selected from each sample, and the number of capillaries was counted manually by 2 pathologists who were unaware of the grouping of

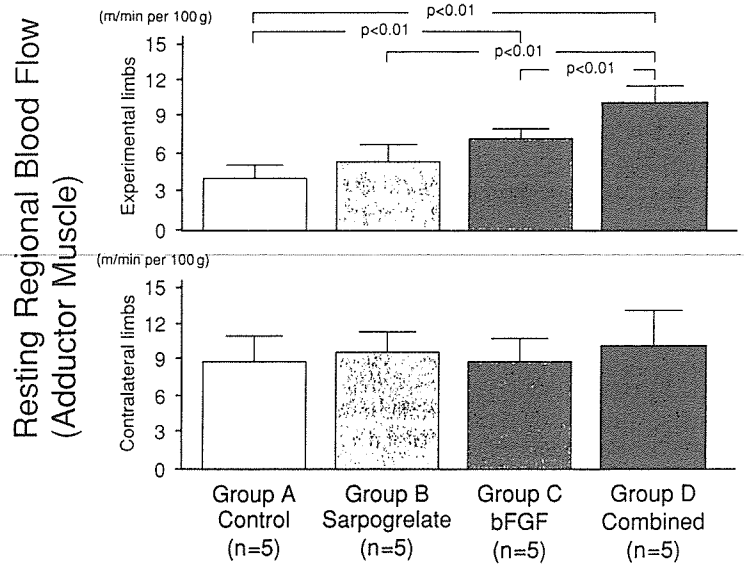

Fig 1. Effect of each treatment on resting hindlimb blood flow measured at 6 weeks after femoral artery extraction. The resting blood flow in the adductor muscles of the experimental (Top panel) and contralateral (Bottom panel) limbs was assessed by color microspheres and compared with the control group. bFGF, basic fibroblast growth factor.

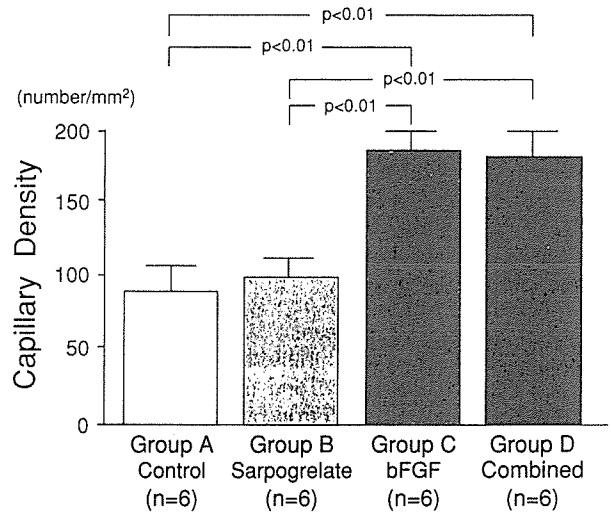

Fig 2. Effect of each treatment on capillary density examined at 6 weeks after femoral artery extraction. The capillary density in the adductor muscles of the experimental limbs was assessed histologically and compared with the control group. bFGF, basic fibroblast growth factor.

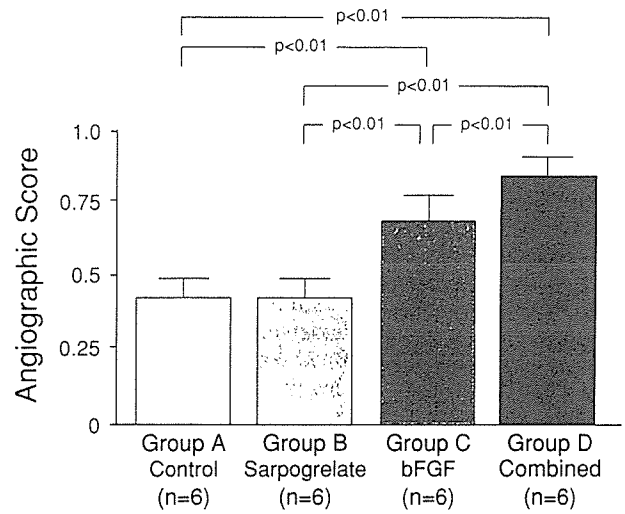

Fig 3. Effect of each treatment on the growth and development of angiographically visible collateral vessels. The angiographic score represents the density of collateral vessels in the medial thigh region of the experimental limb. bFGF, basic fibroblast growth factor.

the rabbits. Finally, the capillary density was calculated as the number of capillaries/mm² of muscle.

Statistical Analysis

Results are expressed as the mean±standard deviation. Differences among groups were determined by 1-way analysis of variance followed by multiple comparisons using the Bonferroni/Dunn's test. All statistical analyses were performed using Statview™ software (Abacus, Calabosus, CA, USA). A p-value <0.05 was considered significant.

Results

There were no deaths of rabbits as a result of the surgical manipulation. We found neither local disorders nor complications attributable to the topical use of sustained-release bFGF.

Regional Blood Flow

The resting regional blood flow was assessed using the colored microspheres as described earlier. In the ischemic adductor muscle, the regional blood flow in group D was the highest among the 4 groups (4.0±0.7, 5.8±1.0, 7.2±0.6, 9.7±2.0 ml/min per 100 g tissue for groups A, B, C and D, respectively; $p<0.01$) (Fig 1). In addition, there was no statistically significant difference between the resting regional blood flow in the right adductor muscle (ischemic) and that in the left adductor muscle (non-ischemic) in group D (9.7±2.0 and 10.4±3.5 ml/min per 100 g tissue, respectively) (Fig 1). No significant differences in the normal hindlimb blood flow in the adductor muscles were observed among the 4 groups (8.6±2.4, 9.3±1.8, 8.8±1.5, 10.4±3.5 ml/min per 100 g tissue for each group) (Fig 1).

Capillary Density

A favorable effect of sustained-release bFGF was shown

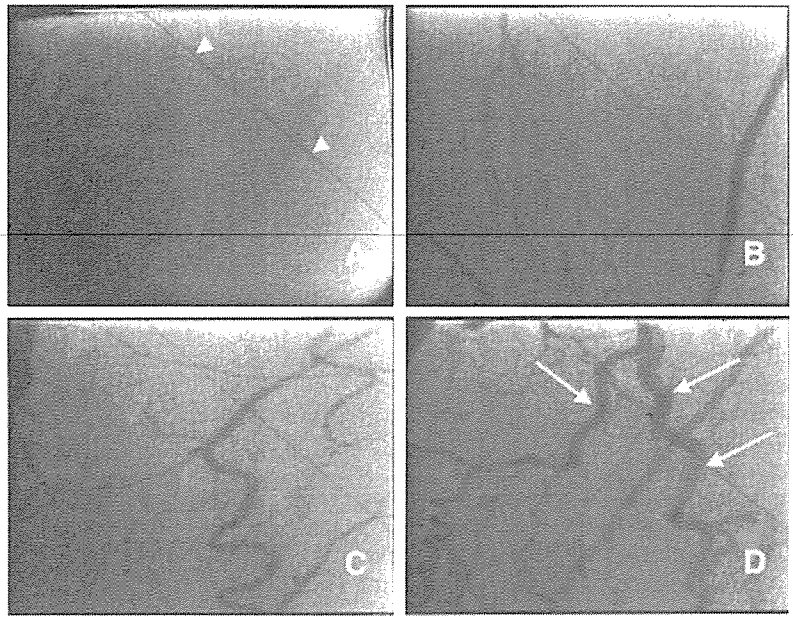

Fig 4. Representative angiographic images of the experimental limb of rabbits treated with sarpogrelate (B), bFGF (C), or a combination of sarpogrelate and bFGF (D). Rabbits with no treatment served as the control (A). The diameter of the reference wire (arrowheads) was 130μm. Imaging field of each microangiogram was 20×20 mm. Note the increased density of collateral vessels in the medial thigh region of rabbits treated with sustained-release bFGF (C, D). A more increased diameter was observed in the rabbits with the combined treatment of bFGF and sarpogrelate (arrows). bFGF, basic fibroblast growth factor.

in terms of capillary proliferation (Fig 2). The adductor muscles of the ischemic hindlimbs were examined histologically 6 weeks after surgery. The mean values of the capillary density in groups treated with sustained-release bFGF were significantly higher than those in groups without bFGF (89±17, 96±12, 181±19, 179±22/mm^2 for groups A, B, C and D; $p<0.01$). The mean value of the capillary density in the adductor muscle of the contralateral non-ischemic hindlimb was 129±18/mm^2. Thus, the capillary density in the ischemic hindlimb of rabbits treated with sustained-release bFGF was significantly higher than that in the non-ischemic hindlimb.

Microangiographic Assessment

Assessment of the number of angiographically visible collateral vessels (the aforementioned angiographic score) showed the highest increase in group D with the combined treatment among the 4 groups (0.41±0.06, 0.42±0.04, 0.68±0.07, 0.79±0.06 for groups A, B, C and D, respectively; $p<0.01$) (Fig 3).

Administration of sustained-release bFGF induced the enlargement of collateral vessels (Figs 4C,D). Importantly, a further vasodilatory effect was observed in the collateral vessels of the rabbits with then additional sarpogrelate treatment.

Discussion

This is the first study demonstrating that an angiogenic therapy aimed at collateral vessel growth and dilation significantly increased collateral blood flow. The results from the present study are in agreement with the conceptual framework of the functional improvement in collateral blood flow. Sustained-release bFGF enhanced angiogenesis and arteriogenesis, and sarpogrelate did not augment angiogenesis and arteriogenesis, but rather dilated collateral vessels with several layers of smooth muscle cells. Thus, angiogenesis, arteriogenesis and the dilation of collateral vessels contributed to augmented collateral blood flow in the rabbit hindlimb following femoral artery removal.

Data from the present study clearly demonstrate that collateral blood flow was the highest in the rabbits with the combined treatment of sustained-release bFGF and sarpogrelate. Collateral blood flow is augmented mainly by arteriogenesis and the dilation of collateral vessels[3] Indeed, Hershey et al have elegantly shown that increases in collateral blood flow do not parallel angiogenesis, but rather arteriogenesis, in a rabbit hindlimb ischemia model! Also, it is well appreciated that vasodilators, such as nitroglycerin, dilate newly developed collateral vessels, and increase collateral blood flow[20]

For the evaluation of arteriogenesis, we used an angiographic score derived from microangiography, which allowed for the visualization of small collateral vessels with diameters greater than 30μm![18,19] The number of angiographically visible collateral vessels may be augmented not only by arteriogenesis, but also by vasodilation of smaller collateral vessels by vasodilatory agents. Thus, microangiograms indirectly reveal the conductance of collateral vessels. Regarding angiogenesis, our findings are intriguing, because the capillary density in the ischemic hindlimb showed a 1.4-fold increase compared with that in the non-ischemic hindlimb. However, it is unclear whether the enhanced angiogenesis favorably contributed to the functional regional blood flow in the ischemic muscle. Furthermore, because capillary density is largely affected by the volume of skeletal myocytes, the cross-sectional area of myocytes must be taken into account.

In the present study, we demonstrated that a single intramuscular injection of gelatin hydrogel microspheres incorporating bFGF (sustained-release bFGF) significantly improved tissue blood flow through angiogenesis and arteriogenesis in a rabbit hindlimb ischemic model. Therapeutic angiogenesis with growth factors has been developed for the treatment of severe PAD[7,8,19] Of the growth factors, bFGF is one of the most potent mitogens regulating the proteins that induce proliferation of a variety of cells and promote the growth and regeneration of organs and tissues in vivo[21] Although the biological half-life of bFGF in its free form is very short, it has been reported that collateral vessel growth can be obtained with multiple injections[8] In the present study, we used a single local injection of sus-

tained-release bFGF and from the significant increase in the number of capillaries and angiographically demonstrable collateral vessels, we confirmed that remarkable collateral growth through angiogenesis and arteriogenesis had occurred. In addition, the sustained-release bFGF induced significant regional blood flow recovery in the ischemic limbs. Because we did not find any local or systemic complications attributable to the topical use of sustained-release bFGF, this treatment would be applicable for critically ill patients with PAD. In the near future, the new treatment reported here may be comparable with other therapeutic modalities such as gene therapy,[22] cell therapy with bone marrow cells,[23] or peripheral blood mononuclear cells.[24]

It is tempting to speculate on the mechanisms for the effectiveness of sarpogrelate for enhancing the collateral blood flow in the present study. As shown in Fig 4, sarpogrelate dilated the collateral vessels, presumably by blockade of the 5-hydroxytryptamine (5-HT) subtype 2A receptor in the vascular smooth muscle cells in the newly developed collateral vessels. The dilation of collateral vessels by serotonin blockers, such as sarpogrelate and ketanserin, has been shown in humans with effort angina.[25,26] Alternatively, the increased collateral blood flow mediated by sarpogrelate blockade of the 5-HT2A receptor possibly augments shear stress at the site of preexistent collateral vessels. Indeed, arteriogenesis is potentiated through amplification of endogenous endothelial signaling mediated by changes in shear stress.[27–29] It may be difficult to determine the relative contribution of sarpogrelate to acute vasodilation or the resultant chronically enhanced arteriogenesis. To this end, a microangiographic study of single administration of sarpogrelate may reveal the favorable vasodilatory effect of this serotonin blocker.[25,26]

In summary, the present study demonstrated that intramuscular administration of a sustained-release form of bFGF stimulated collateral vessel growth, and combined treatment with sarpogrelate produced a further improvement in the hindlimb blood flow of a rabbit model of peripheral arterial insufficiency. These results suggest that the new therapy reported here could stimulate a meaningful improvement in collateral blood flow in patients with PAD.

References

1. Hershey JC, Baskin EP, Glass JD, Hartman HA, Gilberto DB, Rogers IT, et al. Revascularization in the rabbit hindlimb: Dissociation between capillary sprouting and arteriogenesis. *Cadiovasc Res* 2001; **49:** 618–625.
2. Herzog S, Sager H, Khmelevski E, Deylig A, Ito WD. Collateral arteries grow from preexisting anastomoses in the rat hindlimb. *Am J Physiol Heart Circ Physiol* 2002; **283:** H2012–H2020.
3. Fujita M, Tambara K. Recent insights into human coronary collateral development. *Heart* 2003; **90:** 246–250.
4. Heil M, Schaper W. Influence of mechanical, cellular, and molecular factors on collateral artery growth (arteriogenesis). *Circ Res* 2004; **95:** 449–458.
5. Prior BM, Lloyd PG, Ren J, Li H, Yang HT, Laughlin MH, et al. Time course of changes in collateral blood flow and isolated vessel size and gene expression after femoral artery occlusion in rats. *Am J Physiol Heart Circ Physiol* 2004; **287:** H2434–H2447.
6. Isner JM, Pieczek A, Schainfeld R, Blair R, Haley L, Asahara T, et al. Clinical evidence of angiogenesis after arterial gene transfer of phVEGF165 in patient with ischaemic limb. *Lancet* 1996; **348:** 370–374.
7. Rajagopalan S, Mohler ER 3rd, Lederman RJ, Mendelsohn FO, Saucedo JF, Goldman CK, et al. Regional angiogenesis with vascular endothelial growth factor in peripheral arterial disease: A phase II randomized, double-blind, controlled study of adenoviral delivery of vascular endothelial growth factor 121 in patients with disabling intermittent claudication. *Circulation* 2003; **108:** 1933–1938.
8. Baffour R, Berman J, Garb JL, Rhee SW, Kaufman J, Friedmann P. Enhanced angiogenesis and growth of collaterals by in vivo administration of recombinant basic fibroblast growth factor in a rabbit model of acute lower limb ischemia: Dose-response effect of basic fibroblast growth factor. *J Vasc Surg* 1992; **16:** 181–191.
9. Tabata Y, Nagano A, Ikada Y. Biodegradation of hydrogel carrier incorporating fibroblast growth factor. *Tissue Eng* 1999; **5:** 127–138.
10. Iwakura A, Tabata Y, Miyao M, Ozeki M, Tamura N, Ikai A, et al. Novel methods to enhance sternal healing after harvesting bilateral internal thoracic arteries with use of basic fibloblast growth factor. *Circulation* 2000; **102:** III-307–III-311.
11. Ueyama K, Bing G, Tabata Y, Ozeki M, Doi K, Nishimura K, et al. Development of biologic coronary artery bypass grafting in a rabbit model: Revival of a classic concept with modern biotechnology. *J Thorac Cardiovasc Surg* 2004; **127:** 1608–1615.
12. Marui A, Kanematsu A, Yamahara Y, Ozeki M, Doi K, Kushibiki T, et al. Simultaneous application of basic fibroblast growth factor and hepatocyte growth factor to enhance the blood vessels formation. *J Vasc Surg* 2005; **41:** 82–90.
13. Doggrell SA. Sarpogrelate; Cardiovascular and renal clinical potential. *Expert Opin Invest Drugs* 2004; **13:** 865–874.
14. Nagatomo T, Rashid M, Abul Muntasir H, Komiyama T. Functions of 5-HT2A receptor and its antagonists in the cardiovascular system. *Pharmacol Ther* 2004; **104:** 59–81.
15. Wright L, Homans DC, Laxson DD, Dai XZ, Bache RJ. Effect of serotonin and thromboxane A2 on blood flow through moderately well developed coronary collateral vessels. *J Am Coll Cardiol* 1992; **19:** 687–693.
16. Loots W, De Clerck F. 5-Hydroxytryptamine dominates over thromboxane A2 in reducing collateral blood flow by activated platelets. *Am J Physiol* 1993; **265:** H158–H164.
17. Kowallik P, Schulz R, Guth BD, Schade A, Paffhausen W, Gross R, et al. Measurement of regional myocardial blood flow with multiple colored microspheres. *Circulation* 1991; **83:** 974–982.
18. Takeshita S, Isshiki T, Mori H, Tanaka E, Eto K, Miyazawa Y, et al. Use of synchrotron radiation microangiography to assess development of small collateral arteries in a rat model of hindlimb ischemia. *Circulation* 1997; **95:** 805–808.
19. Takeshita S, Rossow ST, Kearney M, Zheng LP, Bauters C, Bunting S, et al. Time course of increased cellular proliferation in collateral arteries after administration of vascular endothelial growth factor in a rabbit model of lower limb vascular insufficiency. *Am J Pathol* 1995; **147:** 1649–1660.
20. Fujita M, McKown DP, McKown MD, Franklin D. Effects of glyceryl trinitrate on functionally regressed newly developed collateral vessels in conscious dogs. *Cardiovasc Res* 1988; **22:** 639–647.
21. Rifkin DB, Moscatelli D. Recent developments in the cell biology of basic fibroblast growth factor. *J Cell Biol* 1989; **109:** 1–6.
22. Morishita R, Aoki M, Hashiya N, Makino H, Yamasaki K, Azuma J, et al. Safety evaluation of clinical gene therapy using hepatocyte growth factor to treat peripheral arterial disease. *Hypertension* 2004; **44:** 203–209.
23. Saigawa T, Kato K, Ozawa T, Toba K, Makiyama Y, Minagawa S, et al. Clinical application of bone marrow implantation in patients with arteriosclerosis obliterans, and the association between efficacy and the number of implanted bone marrow cells. *Circ J* 2004; **68:** 1189–1193.
24. Ishida A, Ohya Y, Sakuda H, Ohshiro K, Higashiuesato Y, Nakaema M, et al. Autologous peripheral blood mononuclear cell implantation for patients with peripheral arterial disease improves limb ischemia. *Circ J* 2005; **69:** 1260–1265.
25. Tanaka T, Fujita M, Nakae I, Tamaki S, Hasegawa K, Kihara Y, et al. Improvement of exercise capacity by sarpogrelate as a result of augmented collateral circulation in patients with effort angina. *J Am Coll Cardiol* 1998; **32:** 1982–1986.
26. Kyriakides ZS, Sbarouni E, Nikolaou N, Antoniadis A, Kremastinos DT. Intracoronary ketanserin augments coronary collateral blood flow and decreases myocardial ischemia during balloon angioplasty. *Cardiovasc Drugs Ther* 1999; **13:** 415–422.
27. Helisch A, Schaper W. Arteriogenesis: The development and growth of collateral arteries. *Microcirculation* 2003; **10:** 83–97.
28. Kersten JR, Pagel PS, Chilian WM, Warltier DC. Multifactorial basis for coronary collateralization: A complex adaptive response to ischemia. *Cardiovasc Res* 1999; **43:** 44–57.
29. Wahlberg E. Angiogenesis and arteriogenasis in limb ischemia. *J Vasc Surg* 2003; **38:** 198–203.

Effects of Monofilament Nylon Coated With Basic Fibroblast Growth Factor on Endogenous Intrasynovial Flexor Tendon Healing

Yoshitaka Hamada, MD, Shinsuke Katoh, MD, Naohito Hibino, MD, Hirofumi Kosaka, MD, Daisuke Hamada, MD, Natsuo Yasui, MD

From the Department of Orthopedics, Institute of Health Biosciences, University of Tokushima Graduate School, Tokushima, Japan; and the Institute for Frontier Medical Sciences, Kyoto University, Kyoto, Japan.

Purpose: We developed a monofilament nylon thread that can release various growth factors to enhance intrinsic reparative processes after flexor tendon injury. We evaluated the properties of this thread *in vitro* and *in vivo*.

Methods: Nylon threads were coated with gelatin that subsequently was cross-linked in glutaraldehyde. The thread was soaked in basic fibroblast growth factor (bFGF) solution (400 μg/mL). Exogenous bFGF in the thread was released constantly over the course of 1 week. The biologic activity of bFGF and the biomechanical strength of the thread were examined *in vitro* and its efficacy was investigated in an *in vivo* rabbit tendon repair model after early flexion exercises. The sutured sites were examined histologically (hematoxylin-eosin, immunohistochemistry, *in situ* hybridization), biochemically (Western blot test), and biomechanically (ultimate load) after surgery.

Results: This gelatin-coated thread absorbed iodine 125–labeled bFGF in a time-dependent manner. The total amount of bFGF absorbed by the thread within the tendon tissue was between 3 and 15 μg depending on the concentration of bFGF solution. Basic fibroblast growth factor protein was delivered selectively—not in the surrounding scar but in the repaired tendon—for 3 weeks. Histologic analysis showed that the cellular density at the repaired site increased in accordance with the expression of bFGF messenger RNA and protein in the tendon. Endogenous bFGF expression seemed to be enhanced transiently by exogenous bFGF during the first few weeks. The epitenon showed a vigorous fibroblastic response to the coated thread and the ultimate load also was increased significantly at 3 weeks after surgery.

Conclusions: This bFGF-coated nylon suture gave excellent results in delivering a drug selectively to tendon; it also induced an increase of biomechanical strength and a thickening of the epitenon layer *in vivo* during a 3-week period, thereby accelerating cellular proliferation, initially peripherally and later centrally. This system may become a therapeutic tool to be used in hand surgery. (J Hand Surg 2006;31A:530–540. Copyright © 2006 by the American Society for Surgery of the Hand.)

Key words: Bioactive monofilament nylon thread, drug delivery system, flexor tendon healing, growth factors, postoperative early active flexion exercises.

Repair of hand flexor tendons often is complicated by the formation of peritendinous adhesions and dehiscence at the repair site.[1,2] Dehiscence at the repair site in the early phase of healing seems to have become a very serious problem because early postoperative exercises are recommended more commonly to prevent adhesions. This could be overcome if it were possible to accelerate tendon healing.[1,3,4]

The tendon healing process via the extrinsic pathway, in which fibroblasts and inflammatory cells from the surrounding tissue and synovial sheath participate, becomes very active in the early phase of

tendon healing.[5] The quality of tissue repaired via the extrinsic pathway, however, is poor, leading to the formation of a scar and adhesions. Therefore the intrinsic pathway seems to be more favorable for the healing process. The epitenon is believed to play an important role in the intrinsic pathway[6] but endotenon tenocytes produce a more mature matrix than the epitenon tenocytes.[7,8] Consequently stimulation of the intrinsic pathway by growth factors is one way to induce an acceleration of flexor tendon healing.[4,9–12] Selection of the growth factor and its appropriate application are very important. We developed a monofilament nylon thread that can release various growth factors into the tendon tissue to stimulate the intrinsic pathway. We used basic fibroblast growth factor (bFGF) in this first trial. In this study we evaluated the properties of the thread and the release of bFGF and its effect on tendon repair using an *in vivo* rabbit model.

Materials and Methods

Development of the Monofilament Nylon Thread

A 4-0 double-needle loop nylon thread was used. First, the hydrophobic character of the threads was reduced by corona electric discharge. Immediately after that the threads were soaked in 10% by weight gelatin (isoelectric point = 5.0 pH) (Nitta Gelatin Inc., Osaka, Japan) containing 2.5 mmol/L glutaraldehyde (GA) at 40°C. This coating process was repeated 3 times. The gelatin coating was cross-linked in GA solution at 4°C for 12 hours. The concentration of GA was determined based on the results of a previous experiment in which we investigated the absorption rate of iodine 125 (^{125}I)–labeled bFGF in the subcutaneous tissue of animals.[13] In this experiment the release of bFGF was set to last 1 week. The rest of the aldehyde groups were blocked by soaking the threads in 0.1-mol/L glycine solution. The threads then were washed 4 times with saline at 4°C for 30 minutes each time. The threads were freeze-dried after freezing at −80°C. Before tendon repair a thread was soaked in 400 μg/mL of bFGF solution for 30 minutes. Recombinant human bFGF (Kaken Pharmaceutical Co., Ltd., Tokyo, Japan) was used.

Properties of the Monofilament Nylon Thread

The amount of bFGF absorbed by the gelatin coating was measured by counting ^{125}I-labeled bFGF. The mechanical strength of the threads and knots was investigated by measuring the ultimate load (each group, n = 4). Ultimate load was defined as the measured load until failure with a support span of 20 mm between the holders of each end of a thread, using an alternating-current servo hydraulic materials testing system (AGS-100D; Shimadzu, Kyoto, Japan) with a 10-kg load cell (maximum, about 100 kg) under displacement control (10 mm/min). Load and displacement data were recorded on a computer and the ultimate force (maximum force that the specimen sustained) was calculated from those data.

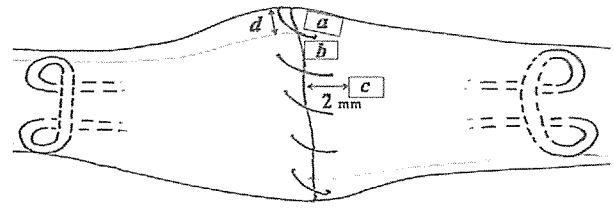

Figure 1. Scored tissue sections (H-E staining). Specimens of repaired tendons were analyzed at ×200 magnification. The thickness of the epitenon layer (*d*) and the cell density (*a, b, c*) were scored as shown.

The biologic activity of bFGF contained in the thread removed 2 days after surgery was assessed based on the proliferation of human fibroblasts cultured in the presence of bFGF(+) threads and bFGF(−) threads.

Reaction of Tendons *In Vivo*

Japanese white rabbits (124 male rabbits weighing 2.5–3 kg) were used. We used the left flexor digitorum fibularis tendons (toe flexors) of the hind limb at the tibial aspect of the ankle.[14] This tendon is similar in size to the human flexor tendon and it is within a fibro-osseous tunnel just as human flexor tendons are. The tendon was cut sharply and sutured according to the modified Kessler method (Y2 method, which is the tendon-suture technique developed by Yoshizu as shown in Fig. 1) using bFGF(+)- or bFGF(−)-coated 4-0 nylon threads as a core suture followed by uncoated 6-0 nylon epitendinous running suture. Early flexion exercises were applied after surgery as reported by Kusano et al.[14] The uncut flexor digitorum profundus also was sutured according to the Y2 method (uncoated threads, n = 4; bFGF[−] threads, n = 3; bFGF[+] threads, n = 4) to investigate the normal tendon reaction to the thread. Repaired tendons were harvested at 1 week (bFGF[−], n = 6; bFGF[+], n = 4), 3 weeks (bFGF[–], n = 6; bFGF[+], n = 6), and 6 weeks (bFGF[−], n = 4; bFGF[+], n = 4) after surgery for histologic analysis. Tendon specimens were fixed in 10% neutral formalin and embedded in paraffin. They were examined under a light microscope after

Table 1. Thickness of the Epitenocytes Layer Measured at Site *d

Normal tendon: 1 week after suture

Normal	Uncoated Thread	bFGF(–) Thread	bFGF(+) Thread
18 ± 7 (n = 5)	63 ± 17 (n = 4)	72 ± 27 (n = 3)	†200 ± 99 (n = 4)

Repaired tendon: 1, 3, and 6 weeks after suture

Group	Normal	1 wk	3 wk	6 wk
bFGF(–)	18 ± 7 (n = 5)	166 ± 62 (n = 6)	291 ± 124 (n = 6)	172 ± 81 (n = 4)
bFGF(+)		275 ± 92 (n = 4)	‡463 ± 138 (n = 6)	238 ± 84 (n = 4)

NOTE. All values are given in micrometers.
*Refers to site labeled d in Figure 1.
†$p < .05$ compared with uncoated and bFGF(–) threads.
‡$p < .05$ compared with bFGF(–) group at 3 weeks.

hematoxylin-eosin (H-E) staining and immunohistochemistry study at 1, 3, and 6 weeks after surgery. The specimens at 3 weeks also were examined using *in situ* hybridization for bFGF messenger RNA (mRNA).

Histology and Immunohistochemistry

The embedded tissues were cut into 4-μm–thick sections. The sections were deparaffinized and processed for H-E staining. Immunohistochemistry was performed using fibroblast growth factor–2 antibody (1:200) (Santa Cruz Biotechnology, CA) and a laboratory kit (Dako LSAB+ kit; Dako, Kyoto, Japan).

In Situ Hybridization

To detect local expression of bFGF mRNA, 5-μm–thick sections were used. Digoxigenin-labeled riboprobes were prepared using a labeling kit (DIG RNA labeling kit; Roche, Mannheim, Germany) and were hydrolyzed in carbonate buffer containing 40 mmol/L of $NaHCO_3$ and 60 mmol/L of Na_2CO_3 to yield about 500–base pair fragments. A 0.3-kb rabbit bFGF fragment (GenBank accession number L-12034) and a 0.3-kilobase rabbit type I collagen fragment were used to generate antisense and sense probes. *In situ* hybridization was performed (Ventana HX system discovery; Ventana Medical Systems, Tucson, AZ) by using a kit (RiboMap Kit; Ventana Medical Systems) with protease 2 for 2 minutes; hybridization was performed at 61°C for 6 hours. Hybrids for bFGF and type I collagen were detected with a kit (BlueMap Kit; Ventana Medical Systems) as described by the manufacturer.

Quantification of Cell Density and Epitenon Thickness

In a blinded fashion tendon specimens were examined at 200-times magnification with a microgrid (Nikon digital camera Dxm 1200; Nikon, Tokyo, Japan). The average thickness of the epitenon layer and the cell density in H-E staining were measured in the areas shown in Figure 1. The thickness of the epitenon and the cell densities of the epitenon and the tendon beneath the epitenon were measured at the area adjacent to the connecting site. The cell density of the tendon was measured at the center of the

Table 2. Changes in Cellular Density at Sites *a, b, c

Time After Repair	Normal	1 W	3 W	6 W
bFGF(–)				
a: Epitenon	474 ± 47 (n = 5)	617 ± 103 (n = 6)	685 ± 56 (n = 6)	707 ± 48 (n = 4)
b: Connected site	—	167 ± 76 (n = 6)	259 ± 162 (n = 6)	632 ± 89 (n = 4)
c: Tendon substance	119 ± 31 (n = 5)	128 ± 36 (n = 6)	138 ± 44 (n = 6)	373 ± 141 (n = 4)
bFGF(+)				
a: Epitenon		688 ± 85 (n = 4)	745 ± 75 (n = 6)	713 ± 63 (n = 4)
b: Connected site		213 ± 63 (n = 4)	†828 ± 260 (n = 6)	725 ± 65 (n = 4)
c: Tendon substance		136 ± 11 (n = 4)	162 ± 77 (n = 6)	‡675 ± 87 (n = 4)

NOTE. Values are given as cells / mm^2.
*Refers to sites labeled a, b, and c in Figure 1.
†$p < .05$ compared with bFGF(–) at 3 weeks.
‡$p < .05$ compared with bFGF(–) at 6 weeks.

Table 3. Changes of the bFGF mRNA-Positive Cell Density

Time After Repair	Normal	3 wk bFGF(–)	3 wk bFGF(+)
a: Epitenon	72 ± 17 (n = 5)	718 ± 48 (n = 4)	*995 ± 213 (n = 4)
b: Tendon substance adjacent to epitenon	22 ± 8 (n = 5)	420 ± 59 (n = 4)	†735 ± 44 (n = 4)
c: Connected site	-	160 ± 43 (n = 4)	190 ± 58 (n = 4)

NOTE. The density of bFGF mRNA-positive cells was measured according to Figure 10A and values are given as cells / mm^2.
*$p < .05$ compared with bFGF(–) at 3 weeks.
†$p < .01$ compared with bFGF(–) at 3 weeks.

repaired tendon 2 mm away from the connecting site. The number of cells found to be positive for express bFGF mRNA by *in situ* hybridization was counted in the areas shown in Figure 9A. Cell density then was averaged and calculated as the mean number of cells within a 1-mm microgrid square of tissue at the repair site. The number of animals that were used at each time point is listed in Tables 1, 2, and 3. Each section was measured twice per tissue section by the different observers and was calculated as the average of 1 sample. One tissue section was selected per 1 experimental sample.

Western Blot Test

Tendons and their surrounding scar tissues were harvested before surgery (normal, n = 3) and at 1, 3, and 6 weeks after surgery (bFGF[–], n = 3; bFGF[+], n = 3). Homogenates were resolved in (RIPA) 1M-Tris-HCl (pH 8.0), 5M-NaCl, 0.5M-EDTA (pH 8.0), 10%-Triton X, 10%-SDS, 10% Na-deoxycholate) buffer (50 mmol/L tris hydroxymethyl aminomethane, pH 7.4, 150 mmol/L NaCl, 1% NP-40, 0.5% sodium deoxycholate, 0.1% sodium dodecyl sulfate) for 7 days at 4°C on a rotating wheel.

The proteins were extracted from the supernatants after centrifugation (12,000 rpm at 4°C for 15 min). Fibroblast growth factor–2 protein was detected using anti–fibroblast growth factor–2 antibody (dilution with 1:250) (Santa Cruz Biotechnology). Protein bands were visualized (ECL Western Blotting Analysis System; Amersham Pharmacia Biotech, Piscataway, NJ). The approximate molecular size of the protein was determined by comparison with molecular size markers (Precision Plus Protein Standards; Bio-Rad Laboratories, Boston, MA). Blotted images were captured and analyzed using imaging software (National Institutes of Health image software, Washington, DC). Relative intensities for protein signals were averaged from the average control value.

Mechanical Strength of the Repaired Tendons

Repaired tendons were harvested at the time of surgery (bFGF[–], n = 6) and at 1 week (bFGF[–], n = 6; bFGF[+], n = 6), 3 weeks (bFGF[–], n = 12; bFGF[+], n = 10), and 6 weeks (bFGF[–], n = 6; bFGF[+], n = 6) after surgery for biomechanic analysis. Tendon specimens were cleaned of soft tissue and preserved frozen in a saline-soaked gauze at −80°C. They were thawed at room temperature 24 hours before the test. They were kept moist during the preparation and testing. In a blinded fashion the ultimate load was measured with the earlier-described method used for thread measurement. Load and displacement data were recorded on a computer and then the ultimate load (maximum force that the specimen sustained) was calculated from those data.

This experimental study was approved by the Institutional Animal Care and Use Committee of our institution. At the end of the experiments all animals were killed with an overdose of sodium pentobarbital. Chi-square analysis, analysis of variance with *post hoc* analysis, and the Student *t* test were used for statistical analysis. The level of statistical significance was set at a p value of less than .05.

Results

Characteristics of the Bioactive Thread

The gelatin coating contributed significantly to increase the ultimate force of the thread and the knot. The strength of the thread increased from 17.3 ± 0.62 N to 23.1 ± 2.9 N. The strength of the knot increased from 5.5 ± 0.5 N to 14.2 ± 2.4 N (Fig. 2). The amount of bFGF absorbed increased in a time-

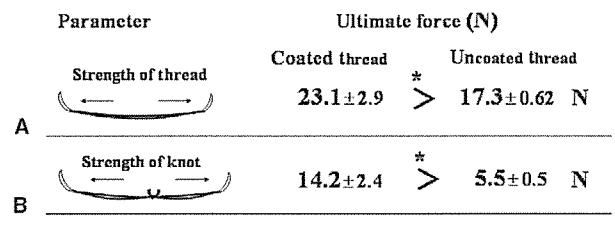

Figure 2. Biomechanical strength of the nylon thread and the coated nylon thread. (A) Ultimate force of the thread. (B) Ultimate force when the knot made with the thread was loosened. Values are given as mean ± SD (n = 4). *$p < .01$

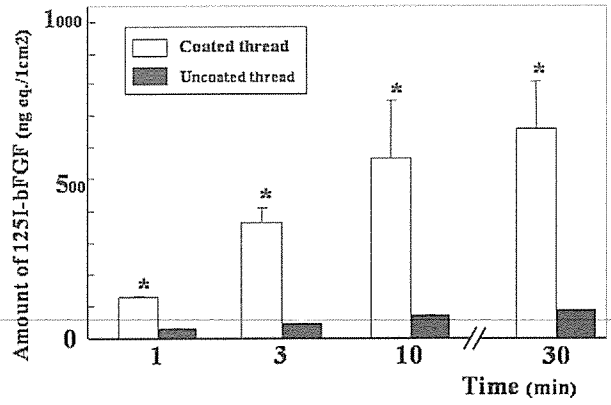

Figure 3. Amount of ^{125}I-bFGF absorbed by coated and uncoated threads as a function of time. The amount of bFGF absorbed increased in a time-dependent manner and reached its maximum level within 30 minutes. Values are given as mean ± SD (n = 3). *p < .01

dependent manner and reached its maximum level within 30 minutes (Fig. 3). The amount of bFGF calculated from the length of the thread within the repaired tendon was 15 μg when soaked in a 2,000-μg/mL bFGF solution and was 3 μg when soaked in a 400-μg/mL solution for 10 minutes. The rate of bFGF released from the thread was almost constant for 7 days. The biologic activity of the bFGF contained in the thread was confirmed based on the increased proliferation of cultured human fibroblasts as the preliminary experiment.

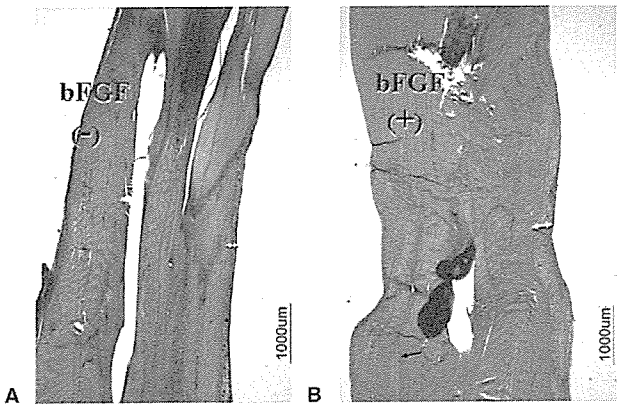

Figure 4. Low-magnification photomicrographs showing the different reactions of normal tendon (uninjured flexor digitorum profundus) at 1 week after surgery with suture using (A) the bFGF(–) thread and (B) the bFGF(+) thread. Note the clearly enhanced thickness of the epitenon layer by bFGF (white arrow). Thickening of the septum that separates the tendon bundles also was enhanced by bFGF (black arrow). The proliferation of tenocytes was observed in the outside layer (epitenon) but not at the center of the tendon substance (endotenon).

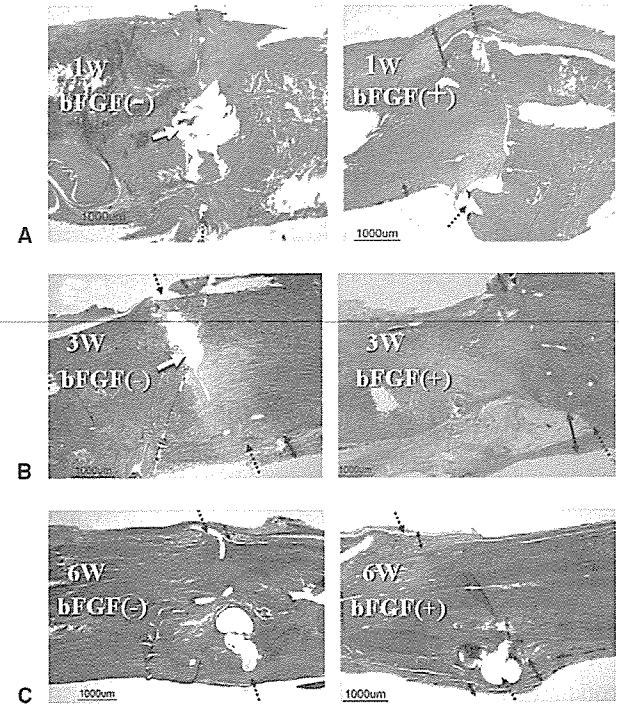

Figure 5. Low-magnification photomicrographs showing repaired tendons using the bFGF(–) and bFGF(+) threads at (A) 1 week, (B) 3 weeks, and (C) 6 weeks after surgery. (A, B) There is increased thickness of the epitenon layer (black arrow). The reparative connection of the detached tendon tissue occurred from the outer epitenon layer (dotted arrow). The center of the repaired site (white arrow) was not completed yet. (B, right) Epitenon thickening and cellular infiltration at the repaired site were enhanced by bFGF at 3 weeks. No gap was observed at the center of the repaired site. (C) At 6 weeks remodeling changes were observed, and cellularity caused by proliferation of tenocytes (endotenon) increased at the center of the repaired site. Newly synthesized collagen and proliferation of tenocytes (endotenon) in the tendon substance were increased. Double dotted arrows indicate the direction of the connecting line.

Histologic Findings

Reaction of normal tendon to the threads (H-E staining). We evaluated the reaction of normal tendon (uncut flexor digitorum profundus) to the bFGF(−) thread and the bFGF(+) thread only at 1 week after surgery to determine the areas that react to this bFGF-releasing system during 1 week (Fig. 4). The proliferation of tenocytes in the center of the tendon (endotenon) was not enhanced. The proliferation of epitenon was enhanced by bFGF and the epitenon layer was significantly thicker ($p < .05$) in the bFGF(+) group in the repaired tendon at 3 weeks and in the normal tendon at 1 week (Table 1).

Tendon repair model (H-E staining). Figure 5 shows a sagittal section of serial changes of the

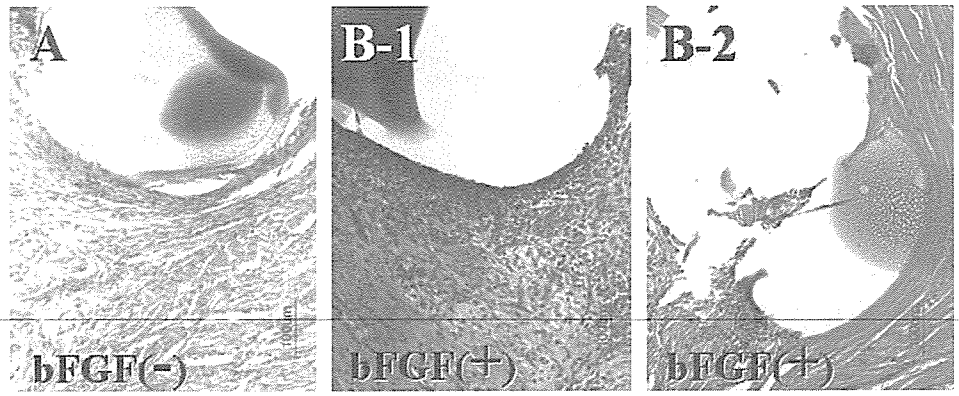

Figure 6. High-magnification photomicrographs showing tissues around the nylon thread in a repaired tendon at 3 weeks after surgery adjacent to the epitenon layer using (A) the bFGF(–) thread and (B, C) the bFGF(+) thread. There was vigorous cellular proliferation adjacent to (B) the epitenon layer but not in (C) the tendon substance in the bFGF(+) group.

repaired tendon at 1, 3, and 6 weeks after surgery. The difference between bFGF(−) thread and bFGF(+) thread at each week was investigated.

At 1 week the proliferation of epitenocytes was vigorous and a reparative connection was observed in the outer layer (epitenocyte layer). This proliferation was enhanced in the bFGF(+) group but the difference from the bFGF(−) group did not reach statistical significance (Tables 1, 2).

At 3 weeks epitenocyte infiltration into the repaired site was observed in the bFGF(−) group, and this infiltration at the connected site was significantly more marked in the bFGF(+) group (Table 2). The thickness of the epitenon layer reached its maximum level at 3 weeks and was significantly greater in the bFGF(+) group (Table 1). Filling of the outer layer of the gap, probably with epitenocytes, was observed in all the groups. A sizable gap, however, still was observed at the center of the sutured site in 4 out of 5 tendons examined in the bFGF(−) group. In the bFGF(+) group these gaps were small and were observed only in 2 out of 5 tendons. The increased thickness of the epitenocyte layer in the bFGF(+) group spread more than 10 mm longitudinally and

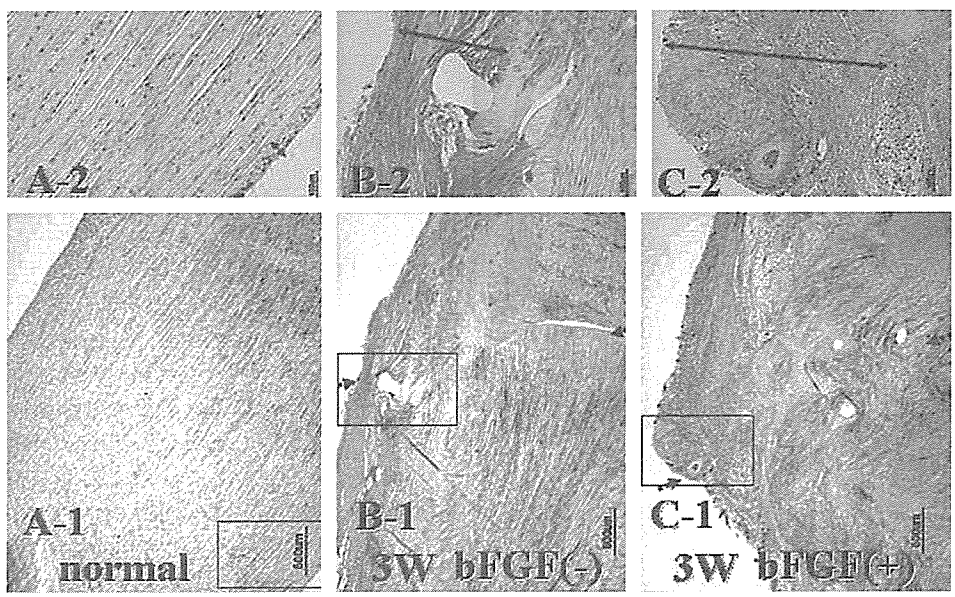

Figure 7. Low-magnification photomicrographs showing bFGF protein in tendon tissue by immunohistochemical analysis. (A) Normal tendon. Few tenocytes and tendon sheath cells expressed bFGF protein in normal tendons. Black arrow, epitenon layer. (B) The bFGF(–) group at 3 weeks after surgery. Transected tendons and repaired tendons showed an increase of bFGF protein, which was expressed dominantly in the epitenon layer. (C) The bFGF(+) group at 3 weeks after surgery. Our bFGF-releasing system enhanced the increase of bFGF protein at the epitenon layer and at the connecting site. Double dotted arrows indicate the direction of the connecting line.

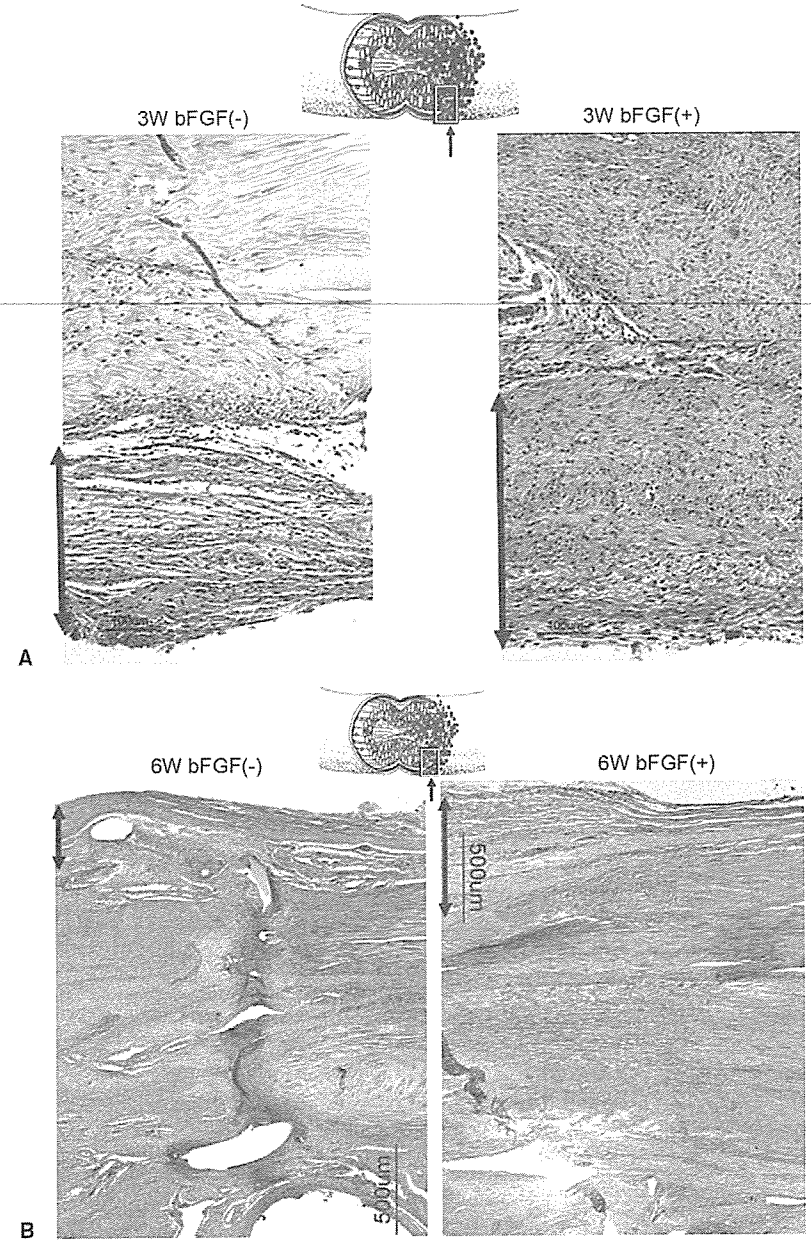

Figure 8. Photomicrographs showing bFGF protein in tendon tissue by immunohistochemical analysis. Counterstaining was performed using hematoxylin to show the distribution of nucleus. (A) At 3 weeks the coincidence between the site showing an increase of bFGF protein and that with high cellularity in which resident tenocytes and infiltrating fibroblasts and inflammatory cells from the epitenon layer concentrated was visible clearly. (B) At 6 weeks bFGF protein was observed to be distributed diffusely throughout the tendon tissue. The difference between bFGF(−) and bFGF(+) was unclear.

the epitenocytes infiltrated the repaired site more vigorously (Table 2).

At 6 weeks remodeling changes were observed and cellularity increased at the center of the tendon. Newly synthesized collagen and proliferation of tenocytes (endotenon) in the tendon substance increased (Table 2).

Therefore, during the synovial tendon healing process cellular proliferation was observed initially in the periphery and later at the center, and this healing was accelerated by bFGF. These serial observations are consistent with the measurements in each section (Tables 1, 2).

Figure 6 shows the reaction around the nylon thread in a repaired tendon at 3 weeks after surgery using the bFGF(−)and bFGF(+) threads. Cellular proliferation adjacent to the epitenon layer was lower in the bFGF(−) group (Fig. 6A). There was

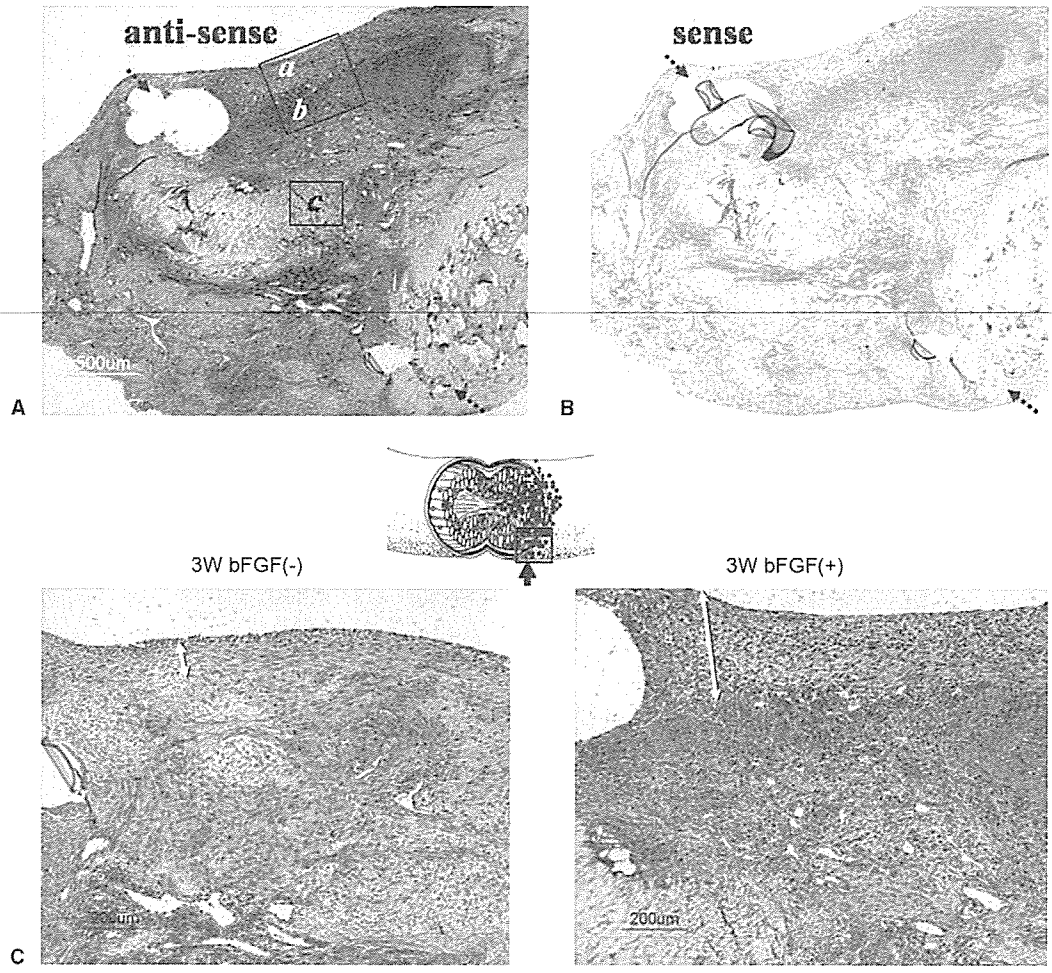

Figure 9. Low-magnification photomicrographs showing (A) antisense and (B) sense pictures of bFGF mRNA expression in a repaired tendon 3 weeks after surgery and suture using the bFGF(+) thread. After tendon injury the expression of bFGF mRNA in the layer of proliferating epitenocytes was detected clearly (*a*). Note the vigorous expression of bFGF mRNA within the tendon substance adjacent to the epitenocytes layer (*b*). The expression of bFGF mRNA was low in the center of the connecting site (*c*). Double dotted arrows indicate the direction of the connecting line. (C) The difference between bFGF(−) and bFGF(+) groups. In the bFGF(−) group epitenocytes dominantly expressed bFGF mRNA. In the bFGF(+) group tenocytes in the tendon tissue adjacent to the epitenon layer also strongly expressed bFGF mRNA. White arrows indicate the epitenon layer.

vigorous cellular proliferation adjacent to the epitenon layer (Fig. 6B) but not in the tendon substance (Fig 6C) in the bFGF(+) group.

Epitenon thickening and cellular infiltration at the repaired site were vigorous within 3 weeks and they were enhanced significantly by bFGF at 3 weeks (Figs 5B, 6; Tables 1, 2). Cellular proliferation within the tendon substance was observed at 6 weeks—much later than in the epitenon layer—and these remodeling reactions also were enhanced significantly by bFGF at 6 weeks (Fig. 5C, Table 2).

Immunohistochemical Study

Positive staining for bFGF was observed in all groups. (Figs. 7, 8) Positive immunoreactivity for bFGF mainly was observed diffusely at the matrix; therefore it was difficult to quantify.

In uninjured intrasynovial flexor tendons the amount of constitutively expressed bFGF was low, but it was expressed dominantly in the epitenon layer (Fig. 7A).

Up to 3 weeks after tendon injury the increase of bFGF immunoreactivity was in accordance with the infiltration of fibroblasts and inflammatory cells surrounding the repaired site (Fig. 7B). The immunoreactivity against bFGF was more marked in the high cellular density area in the bFGF(+) group (Figs. 7C, 8A).

At 6 weeks after tendon repair (Fig. 8B) bFGF protein was observed diffusely throughout the tendon

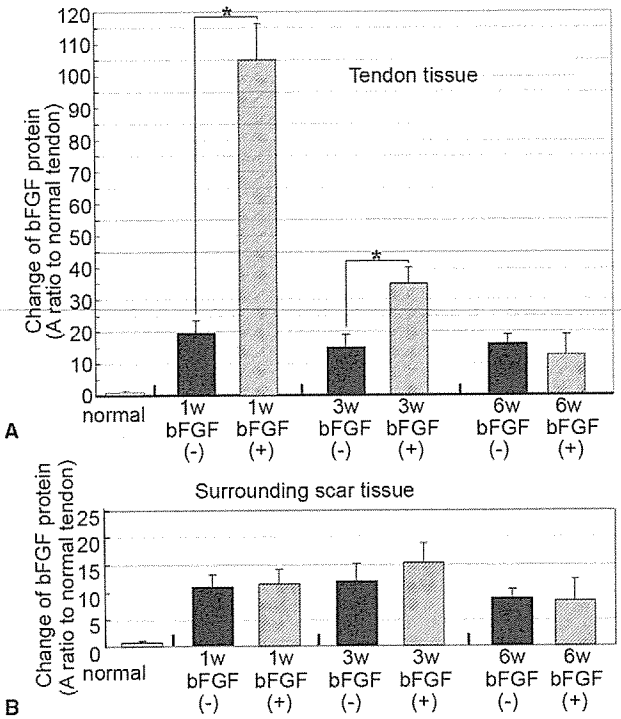

Figure 10. (A) Serial changes in the amount of bFGF protein detected in the repaired tendon tissues. Basic fibroblast growth factor protein increased from 1 to 6 weeks after surgery; it was significantly higher in the bFGF(+) group compared with the bFGF(−) group at 1 and 3 weeks after surgery. There was no significant difference between the groups at 6 weeks. Mean ± SD (n =3). *p < .01. (B) The serial changes in the amount of bFGF protein detected in the surrounding scar tissue corresponding to repaired tendon tissue. The amount of bFGF was much smaller in the surrounding tissue compared with the repaired tendon tissue. These results imply that bFGF(+) thread released bFGF into the tendon tissue selectively. There was no significant difference between them at each week analyzed. Values are given as mean ± SD (n=3).

tissue. The difference in immunoreactivity against bFGF between the bFGF(−) and bFGF(+) groups was not clear.

In Situ Hybridization Study

Figure 9 shows bFGF mRNA expression in the repaired tendon 3 weeks after suture using the bFGF(+) thread. The positive reaction that was not seen on the background sense probe picture but was seen on the antisense probe picture shows the location of bFGF mRNA expression (Fig. 9A). The corresponding sense probes gave no signal in sections used for *in situ* hybridization (Fig. 9B). In the bFGF(−) group epitenocytes dominantly expressed bFGF mRNA; in the bFGF(+) group tenocytes in the tendon tissue adjacent to the epitenon layer also strongly expressed bFGF mRNA (Fig. 9C). Endogenous bFGF mRNA expression was enhanced significantly by the exogenous bFGF-releasing system in the tendon tissue adjacent to the epitenon layer and in epitenocytes at 3 weeks (Table 3).

Western Blot Test

The serial changes in the amount of bFGF protein detected in the repaired tendon tissues are shown in Figure 10A. The amount of bFGF protein in the bFGF(+) group was significantly higher compared with the bFGF(−) group at 1week. The difference became smaller at 3 weeks and there was no significant difference at 6 weeks.

The serial changes in the amount of bFGF protein detected in the surrounding scar tissue are shown in Figure 10B. The amount of bFGF was much lower in the surrounding tissue compared with the repaired tendon tissue and was not different among the tissues examined. These results imply that our system released bFGF into the tendon tissue selectively.

Mechanical Strength

Serial changes in the ultimate load immediately after and at 1, 3, and 6 weeks after surgery in the bFGF(−) and bFGF(+) groups are shown in Figure 11. No decrease of the ultimate load of the repaired tendon

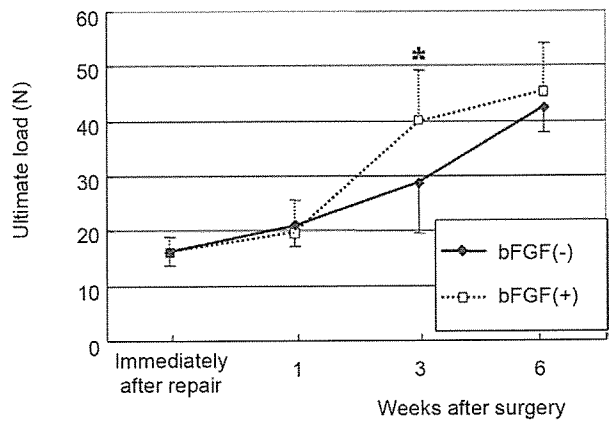

Figure 11. Serial changes in the ultimate load of the repaired tendon immediately after and at 1, 3, and 6 weeks after surgery. The ultimate load of the repaired tendon began to increase from 1 week after surgery; it was significantly higher in the bFGF(+) group compared with the bFGF(−) group at 3 weeks after surgery. There was no significant difference between the groups at other time points. Values are given as mean ± SD. Immediately after surgery: bFGF(−), n = 6. At 1 week after surgery: bFGF(−), n = 6; bFGF(+), n = 6. At 3 weeks after surgery: bFGF(−), n = 12; bFGF(+), n = 10. At 6 weeks after surgery: bFGF(−), n = 6; bFGF(+), n = 6. *p < .05 compared with the bFGF(−) group.

as a result of softening was observed at 1 week after surgery. At 3 weeks the ultimate load in the bFGF(+) group was 35% higher compared with the bFGF(−) group ($p < .05$). There was no significant difference at 1 and 6 weeks.

Discussion

As described in this study the gelatin-coated nylon thread we have developed may become an excellent drug delivery system for use in tendon repair. Our system differs from the nonabsorbable braided polyester thread covalently binding a biologically active peptide (Mersilene) reported previously.[15] Our system has 2 main characteristics: the thread is a monofilament nylon and the duration of the gradual release of bioactive factors can be adjusted by changing the concentration of GA. This growth factor–releasing thread system is intended to enhance intrinsic healing selectively.

We used bFGF because it has been shown to participate in tendon repair.[16] Basic fibroblast growth factor is well known to stimulate angiogenesis, cellular proliferation, chemotaxis, and collagen and fibronectin synthesis.[12,17,18] Because platelet-derived growth factors such as transforming growth factor–beta and platelet-derived growth factor are well known to cause Dupuytren's disease, we must monitor patients carefully for side effects such as increased tendon adhesion and contracture of the hand.[19–24]

In most cases of failure during early postoperative exercises, failure occurs within the first few weeks. Therefore the first 3 weeks are important for the efficacy of early postoperative exercises. Endogenous bFGF expression was observed predominantly in the extrinsic process and at the epitenon layer in the intrinsic process as previously reported.[16] It has been shown that it takes 3 weeks for tendon healing to enter the fibroblastic phase after the acute-inflammatory phase.[1] During these 3 weeks matrix synthesis and angiogenesis reach their maximum levels,[25–27] and mechanical strength begins to increase.[27] We have prepared suture that releases bFGF during 1 week or for up to 3 weeks, but we used the former in this experiment. We plan to compare the 2 different sutures in another study.

The present *in vivo* study showed that this bFGF-releasing system enhanced epitenon thickening at the initial stage and cellular proliferation at the connecting site at a later stage, thereby enhancing the mechanical strength of the tendon by the third week after surgery. The initial reaction occurs at the epitenon layer, and by the third week matrix synthesis and angiogenesis reach their maximum levels and mechanical strength begins to increase.[25–27] Our system may have beneficial effects on this cascade. In the early phase of tendon healing cellular proliferation and infiltration, which degrade tendon fibers, seemed important for tendon healing because these reactions constitute a serial cascade leading to the remodeling of the repaired tendon.

The results of the present study also show that our system seems to enhance the upregulation of bFGF at the transcription and translation levels during the first few weeks after tendon injury. These results suggest that exogenous bFGF released at the initial stage after tendon repair may enhance the expression of endogenous bFGF for at least the first few weeks after surgery. This upregulation may be transient because the amount of bFGF protein in the bFGF(+) group was not higher than that in the bFGF(−) group at 6 weeks, as shown by Western blot analysis.

In the intrasynovial tendon healing process the constitutive expression of bFGF mRNA and protein was low in the epitenon. Tendon laceration was shown to enhance the increase of bFGF mRNA and protein in accordance with the site of proliferation in the epitenon and the infiltration of fibroblasts and inflammatory cells surrounding the repair site up to the third week. At 6 weeks bFGF protein was observed to be distributed diffusely throughout the tendon. Basic fibroblast growth factor expression increased up to 6 weeks after surgery in the bFGF(−) group, but protein expression at the translation level seemed to begin to decrease before the sixth week in the bFGF(+) group. Further studies are necessary to clarify the correlation between exogenous bFGF and intrinsic bFGF expression.

Makoto Ozeki, PhD, Yu Kimura, PhD, and Yasuhiko Tabata, MD, also contributed to this manuscript.

Received for publication July 15, 2005; accepted in revised form December 7, 2005.

No benefits in any form have been received or will be received from a commercial party related directly or indirectly to the results of this article.

Corresponding author: Yoshitaka Hamada, Department of Orthopedics, Tokushima University 318-15 Kuramoto-cho, Tokushima 770-8503, Japan; e-mail: hamada-yoshitaka@umin.ac.jp

0363-5023/06/31A04-0003$32.00/0

doi:10.1016/j.jhsa.2005.12.003

References

1. Beredjiklian PK. Biologic aspects of flexor tendon laceration and repair. J Bone Joint Surg 2003;85A:539–550.
2. Gelberman RH, Boyer MI, Brodt MD, Winters SC, Silva MJ. The effect of gap formation at the repair site on the strength and excursion of intrasynovial flexor tendons. An experimental study on the early stages of tendon-healing in dogs. J Bone Joint Surg 1999;81A:975–982.
3. Boyer MI, Goldfarb CA, Gelberman RH. Recent progress in flexor tendon healing. The modulation of tendon healing with rehabilitation variables. J Hand Ther 2005;18:80–85.
4. Silva MJ, Boyer MI, Gelberman RH. Recent progress in flexor tendon healing. J Orthop Sci 2002;7:508–514.
5. Khan U, Edwards JC, McGrouther DA. Patterns of cellular activation after tendon injury. J Hand Surg 1996;21B:813–820.
6. Gelberman RH, Steinberg D, Amiel D, Akeson W. Fibroblast chemotaxis after tendon repair. J Hand Surg 1991;16A: 686–693.
7. Fujita M, Hukuda S, Doida Y. The effect of constant direct electrical current on intrinsic healing in the flexor tendon in vitro. An ultrastructural study of differing attitudes in epitenon cells and tenocytes. J Hand Surg 1992;17B:94–98.
8. Fujita M, Hukuda S, Doida Y. Experimental study of intrinsic healing of the flexor tendon: collagen synthesis of the cultured flexor tendon cells of the canine. Nippon Seikeigeka Gakkai Zasshi 1992;66:326–333.
9. Hsu C, Chang J. Clinical implications of growth factors in flexor tendon wound healing. J Hand Surg 2004;29A:551–563.
10. Thomopoulos S, Harwood FL, Silva MJ, Amiel D, Gelberman RH. Effect of several growth factors on canine flexor tendon fibroblast proliferation and collagen synthesis in vitro. J Hand Surg 2005;30A:441–447.
11. Duffy FJ Jr, Seiler JG, Gelberman RH, Hergrueter CA. Growth factors and canine flexor tendon healing: initial studies in uninjured and repair models. J Hand Surg 1995; 20A:645–649.
12. Molloy T, Wang Y, Murrell G. The roles of growth factors in tendon and ligament healing. Sports Med 2003;33:381–394.
13. Ozeki M, Tabata Y. In vivo promoted growth of mice hair follicles by the controlled release of growth factors. Biomaterials 2003;24:2387–2394.
14. Kusano N, Yoshizu T, Maki Y. Experimental study of two new flexor tendon suture techniques for postoperative early active flexion exercises. J Hand Surg 1999;24B:152–156.
15. Rohrich RJ, Trott SA, Love M, Beran SJ, Orenstein HH. Mersilene suture as a vehicle for delivery of growth factors in tendon repair. Plast Reconstr Surg 1999;104:1713–1717.
16. Chang J, Most D, Thunder R, Mehrara B, Longaker MT, Lineaweaver WC. Molecular studies in flexor tendon wound healing: the role of basic fibroblast growth factor gene expression. J Hand Surg 1998;23A:1052–1058.
17. Tang JB, Xu Y, Ding F, Wang XT. Tendon healing in vitro: promotion of collagen gene expression by bFGF with NF-kappaB gene activation. J Hand Surg 2003;28A:215–220.
18. Chan BP, Fu S, Qin L, Lee K, Rolf CG, Chan K. Effects of basic fibroblast growth factor (bFGF) on early stages of tendon healing: a rat patellar tendon model. Acta Orthop Scand 2000;71:513–518.
19. Serini G, Gabbiani G. Mechanisms of myofibroblast activity and phenotypic modulation. Exp Cell Res 1999;250:273–283.
20. Vaughan MB, Howard EW, Tomasek JJ. Transforming growth factor-beta1 promotes the morphological and functional differentiation of the myofibroblast. Exp Cell Res 2000;257:180–189.
21. Bayat A, Watson JS, Stanley JK, Alansari A, Shah M, Ferguson MW, Ollier WE. Genetic susceptibility in Dupuytren's disease. TGF-beta1 polymorphisms and Dupuytren's disease. J Bone Joint Surg 2002;84B:211–215.
22. Chang J, Thunder R, Most D, Longaker MT, Lineaweaver WC. Studies in flexor tendon wound healing: neutralizing antibody to TGF-beta1 increases postoperative range of motion. Plast Reconstr Surg 2000;105:148–155.
23. Alman BA, Naber SP, Terek RM, Jiranek WA, Goldberg MJ, Wolfe HJ. Platelet-derived growth factor in fibrous musculoskeletal disorders: a study of pathologic tissue sections and in vitro primary cell cultures. J Orthop Res 1995; 13:67–77.
24. Terek RM, Jiranek WA, Goldberg MJ, Wolfe HJ, Alman BA. The expression of platelet-derived growth-factor gene in Dupuytren contracture. J Bone Joint Surg 1995;77A:1–9.
25. Gelberman RH, Chu CR, Williams CS, Seiler JG 3rd, Amiel D. Angiogenesis in healing autogenous flexor-tendon grafts. J Bone Joint Surg 1992;74A:1207–1216.
26. Gelberman RH, Khabie V, Cahill CJ. The revascularization of healing flexor tendons in the digital sheath. A vascular injection study in dogs. J Bone Joint Surg 1991;73A:868–881.
27. Gelberman RH, Siegel DB, Woo SL, Amiel D, Takai S, Lee D. Healing of digital flexor tendons: importance of the interval from injury to repair. A biomechanical, biochemical, and morphological study in dogs. J Bone Joint Surg 1991; 73A:66–75.

Key Engineering Materials Vols. 309-311 (2006) pp. 965-968
online at http://www.scientific.net

BMP-2 Dose-response and Release Studies in Functionally Graded HAp

Junichi Tazaki[1,a], Toshiyuki Akazawa[2,b], Masaru Murata[1,c],
Masaya Yamamoto[3], Yasuhiko Tabata[3], Ryota Yoshimoto[1], Makoto Arisue[1]

[1]Oral and Maxillofacial Surgery, School of Dentistry, Health Sciences University of Hokkaido, Kanazawa 1757, Tobetsucho, Ishikarigun 061-0293, Japan
[2]Hokkaido Industrial Research Institute, Nishi-11, Kita-ku, Sapporo 060-0819, Japan
[3]Research Center for Biomedical Engineering, Kyoto University, 53 Kawahara-cho Shogoin, Sakyo-ku, Kyoto 606, Japan

[a]j-tazaki@hoku-iryo-u.ac.jp, [b]akazawa@hokkaido-iri.go.jp, [c]murata@hoku-iryo-u.ac.jp

Keywords: BMP-2, Dose-response, Release, Functionally graded HAp

Abstract. Hydroxyapatite (HAp) has been used as a biomaterial for hard tissues. Critical characteristics of biomaterials will include surface geometry, hydrophobicity and hydrophilicity, crystallinity, biodegradation rates, and release pharmacokinetics (PK) of incorporated molecules such as BMP-2. Optimizing BMP-2 for clinical application may be dependent on localized sustained release from biomaterials. We forcused on *in vivo* local BMP-2 PK and bone induction in two ceramics systems, based on different surface structures. The functionally graded apatites (fg-HAp) was designed by the step-wise calcinations and partial dissolution-precipitation methods. We estimated the *in vivo* release profile of ^{125}I-labeled BMP-2 from fg-HAp and the dose response of bone induction by BMP-2 in the back subcutis histologically. Bulk-HAp (b-HAp) by only the step-wise calcinations was prepared as a control. The amount of BMP-2 remaining in the fg-HAp at 1 day after implantation was 83.8%, while that was 34.6% in the b-HAp. Moreover, ectopic bone formation were found surely in the fg-HAp/BMP-2 (0.5 μ g) system at 3 weeks, not in the b-HAp/BMP-2 system. By using fg-HAp, it is likely that an extremely low dose of BMP-2 is enough to enhance bone induction if BMP-2 is appropriately delivered to the site of action.

Introduction

Bone grafting and bone substitutes are required in many orthopedic and dental indication such as spine fusion, revision of hip prostheses, non-healing fractures, or the filling of large bone defects [1-3]. Autologous bone is still the gold standard in bone reconstructive surgery, because it has osteoconductive and osteoinductive properties. However, harvesting autografts from the iliac crest is often associated with complications such as pain and infections. Furthermore, the harvested quantity of bone autograft (about 20 cm^3) limits its clinical application to small-sized defects. The

viability of autografts after transplantation has also been questioned due to the absence of blood supply [1]. Recent *in vivo* studies have shown that materials should exhibit two features in order to induce ectopic bone: (i) a microporous surface and (ii) a macroporous structure [4,5]. Hydroxyapatite (HAp) has been used as a biomaterial for hard tissues, because of its excellent biocompatibility and osteoconduction. As is well-known, hydroxyapatite (HAp: $Ca_{10}(PO_4)_6(OH)_2$) with hexagonal crystal structure has excellent characteristics for adsorbing biopolymers such as proteins and viruses, which are originated from biocompatibility. From the viewpoint of engineering application, much effort has been made to use HAp as an adsorbent capable of sustained bioactivity for high performance liquid chromatography. Critical characteristics of biomaterials will include surface geometry, hydrophobicity and hydrophilicity, crystallinity, biodegradation rates, and release pharmacokinetics (PK) of incorporated molecules such as BMP-2. Optimizing BMP-2 for clinical application may be dependent on localized sustained release from biomaterials. We forcused on *in vivo* local BMP-2 PK and bone induction in two ceramics systems, based on different surface structures.

Materials and Method

Cortical bones of bovine femur (Holstein, bull, Hokkaido, Japan) were used as starting materials. Spongy and cortical bones in bovine femur were used as starting materials and calcined at 800℃ by the step-wise calcinations to obtain bulk-HAp (b-HAp). The spongy b-HAp was partially dissolved in HNO_3 solution, and the cortical b-HAp was completely dissolved in the other HNO_3 solution. After the two solution were mixed, the PH of the sample solution was carefully adjusted to less than 10.5 by adding NH_4OH aqueous solution, after which the sample solution was aged at 25℃ and the same pH for 24h to reprecipitate HAp (r-HAP). The modified spongy b-HAp was filtrated and dried to fabricate the functionally graded HAp (fg-HAp) ceramics. The fg-HAp ceramics were characterized by the pore sizes of 100~600 μ m, porosities of 70~80%, and small amounts of metal ions. SEM photographs of the fg-HAp showed spherical moss-like grains of about 1.0 μ m in size, which consisted of about 10-nm r-HAp microcrystals [6] (Fig.1). Bulk-HAp (b-HAp) were prepared as control.

BMP-2 release study: Human recombinant BMP-2 (BMP-2) was supplied from Yamanouchi Pharmaceutical Co., Tokyo, Japan. The fg-HAp ($3 \times 3 \times 3$mm) and b-HAp ($3 \times 3 \times 3$mm) containing 0.5 μ g of ^{125}I-labeled BMP-2 were implanted into the back subcutis of 6 week-age female ddY mice. At different time intervals, mice were sacrificed. The skin on the back of mice around the implanted or injected site of BMP-2 was cut into a strip of $3 \times 5cm^2$ and the corresponding facia was thoroughly wiped off with a filter paper to absorb ^{125}I-labeled BMP-2. The radioactivity of HAp remaining, excised skin, and filter paper was measured on the gamma counter to assess the time profile of BMP-2 retention. Measurement of the radioactivity in the other parts of

body, such as blood, heart, lung, thymus, thyroid, liver, spleen, gastrointestine, kidney, and carcass, was made to reveal no accumulation of BMP-2 in any specific organ. Measurement of the radioactivity of the standard was made together with experimental samples at each sampling time (1, 3, 5, 7, 14, 28 day after implamtation). The *in vivo* release profile was assessed based on the radioactivity ratio of samples to the standard [7].

BMP-2 dose-response study: The fg-HAp (3×3×3mm) and b-HAp (3×3×3mm) containing 0.05, 0.1, 0.3, 0.5, 1.0, 5.0 μg of BMP-2 were implanted into the back subcutis of 4 week old Wister rats (Fig.2) [8]. At 3 weeks after implantation, the ceramics were explanted (Fig.3), fixed with 10 vol% neutral formalin solution, dehydrated with ethanol, and embedded in paraffin. The fixed tissues were cross-sectioned to 4 μm thickness with a microtome and stained with Mayer's haematoxylin-eosin (H-E) solution. The histological sections were viewed with an optical microscope.

Result

BMP-2 release study: Fig.4 shows the *in vivo* decrement patterns of BMP-2 from the implamted site of BMP-2-incorporating fg-HAp or b-HAp. The initial BMP-2 dose was 0.5 μg per HAp. As can been seen, BMP-2 was gradually released with time from both HAps. The amount of BMP-2 remaining in the fg-HAp at 1 day after implantation was 83.8%, while that was 34.6% in the b-HAp. It is apparent that fg-HAp/BMP-2 system prolonged *in vivo* BMP-2 retention. After 7 days, there was no significant difference between fg-HAp and b-HAp.

BMP-2 dose-response study: Ectopic bone induction occurred in the fg-HAp/BMP-2 (0.5, 1.0, 5.0 μg) system at 3 weeks, while only in the b-HAp/BMP-2 (5.0 μg), bone induction was found.

Discussion

The osteoinductive properties of BMP-2 are well-documented and have been shown with different carriers by using various animal models. Material properties such as composition, geometry, porosity, size, and microstructure have been reported as critical parameters for bone induction. Ripamoti et al. showed that implant geometry is crucial for bone inductivity [9]. The differences in initial BMP-2 release were presumably due to differences in the available surface area and geometry between fg-HAp and b-HAp. Excellent bone induction in the fg-HAp/BMP-2 system might result in the increase of BMP-2 affinity/binding sites and artificial nano-micro pores. Losing 65% of the BMP-2 dose until 1 day in the b-HAp/BMP-2 system should not be a desirable PK for bone induction. The results also suggest that the retention amount of BMP-2 must be highly enough to induce ectopic bone formation, compared to b-HAp/BMP-2 system.

Summary

Specific nano-micro structures and degradation of fg-HAp is more effective for both BMP-2 retention and bone induction, compared to b-HAp, in the ectopic model. By using fg-HAp, it is likely that an extremely low dose of BMP-2 is enough to enhance bone induction if BMP-2 is appropriately delivered to the site of action. Our fg-HAp ceramics is well designed, biomaterial for bone induction, and a safe and practical delivery system of BMP-2 may be realized in near future.

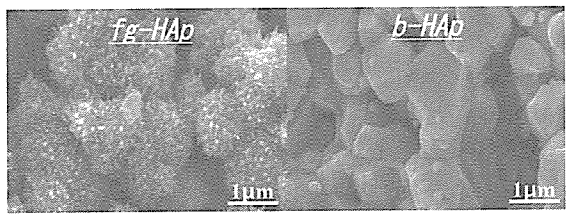

Fig.1 SEM photographs

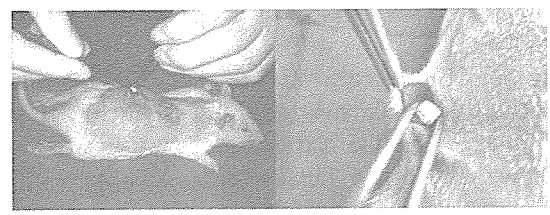

Fig.2 Bioassay model. Implantation

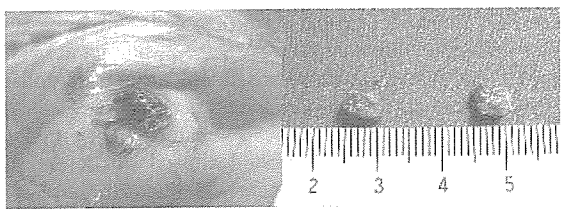

Fig.3 Explantation

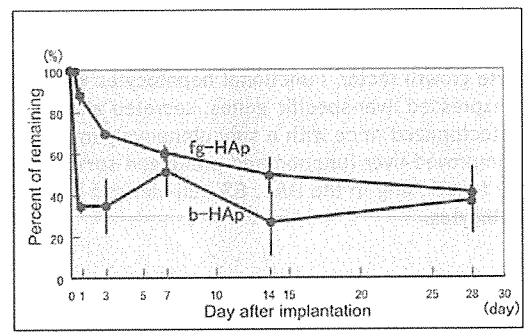

Fig. 4 *In vivo* release of BMP-2 from HAp blocks with or without functionally graded treatments

References

[1] H.Burchardt : Orthop. Clin. North. Am., Vol. 18 (1987), p.187

[2] N.Kubler, C.michel, J.Zoller, J.Bill, J.Muhling and J.Reuther : J. Craniomaxillofac. Surg., Vol. 23 (1995), p.337

[3] F.Taddei, M.Viceconti, M.Manfrini and A.Toni : Proc. Inst. Mech. Eng., Vol. 216 (2002), p.95

[4] H.Yuan, Z.Yang, Y.Li, X.Zhang, JD. de Bruijin and K. de Groot : J. Mater. Sci. Mater. Med., Vol. 9 (1998), p.723

[5] P.Habibovic, H.Yuan, CM. van der Valk, G.meijer, CA. van Blitterswijk and K.de Groot : Biomaterials, Vol. 26 (2005), p.3565

[6] T.Akazawa, M.Kobayashi : Journal of the Ceramic Society of Japan, Vol. 104 (1996), p.284

[7] M.Yamamoto, Y.Tabata and Y.Ikada : J. Biomater. Sci. Polymer Edn., Vol. 9 (1998), p.439

[8] E.A.Wang, V.Rosen, J.S.D'Alessandro, M.Bauduy, P.Cordes, T.Harada, D.I.Israel, R.M.Hewick, K.M.Kerns, P.Lapan, D.P.Luxenberg, D.Mcquaid, I.K.Moutsatsos, J.Nove and J.M.wozney : Proc. Natl. Acad. Sci. USA, Vol. 87 (1990), p.2220

[9] U.Ripamonti, J.Crooks, A,Kirbride : South Afr. J. Sci., Vol. 95 (1999), p.335

nature biotechnology

Reversal of mouse hepatic failure using an implanted liver-assist device containing ES cell–derived hepatocytes

Alejandro Soto-Gutiérrez[1], Naoya Kobayashi[1], Jorge David Rivas-Carrillo[1], Nalu Navarro-Álvarez[1], Debaio Zhao[2], Teru Okitsu[3], Hirofumi Noguchi[3], Hesham Basma[4], Yashuhiko Tabata[5], Yong Chen[1], Kimiaki Tanaka[1], Michiki Narushima[1], Atsushi Miki[1], Tadayoshi Ueda[6], Hee-Sook Jun[7,8], Ji-Won Yoon[7], Jane Lebkowski[9], Noriaki Tanaka[1] & Ira J Fox[4]

Severe acute liver failure, even when transient, must be treated by transplantation and lifelong immune suppression. Treatment could be improved by bioartificial liver (BAL) support, but this approach is hindered by a shortage of human hepatocytes. To generate an alternative source of cells for BAL support, we differentiated mouse embryonic stem (ES) cells into hepatocytes by coculture with a combination of human liver nonparenchymal cell lines and fibroblast growth factor-2, human activin A and hepatocyte growth factor. Functional hepatocytes were isolated using albumin promoter–based cell sorting. ES cell–derived hepatocytes expressed liver-specific genes, secreted albumin and metabolized ammonia, lidocaine and diazepam. Treatment of 90% hepatectomized mice with a subcutaneously implanted BAL seeded with ES cell–derived hepatocytes or primary hepatocytes improved liver function and prolonged survival, whereas treatment with a BAL seeded with control cells did not. After functioning in the BAL, ES cell–derived hepatocytes developed characteristics nearly identical to those of primary hepatocytes.

Acute liver failure can be a lethal condition requiring treatment by liver transplantation. It is frequently reversible, however, and many patients recover with conventional medical support. But because the natural history of acute failure varies widely, even transient hepatic failure, when severe, must be treated by transplantation and lifelong immune suppression[1]. The shortage of donor livers, high cost and requirement for immunosuppression limit the use of this therapeutic modality. Treatment of hepatic failure can be improved by methods for temporary hepatic support. For example, in patients with fulminant liver failure, auxiliary liver transplants can be removed or allowed to undergo rejection when native liver function recovers. This form of therapy is also limited by the shortage of donor organs and by the risks associated with major surgery in the sickest patients[1,2]. In addition, continuous hemodiafiltration with plasma exchange and albumin dialysis improve some parameters of hepatic function and are currently used as temporary support for many patients with acute liver failure[3–5], although improved survival has been difficult to document.

BAL[6,7] devices contain active hepatocytes that remove toxins from the blood and supply physiologically active molecules important for recovery of hepatic function. Although BALs have successfully bridged patients to organ transplantation, this technology has been limited by the lack of human livers as a source of hepatocytes. Potential alternative sources of hepatocytes include porcine hepatocytes[8–10], immortalized human hepatocytes[11], ES cell–derived hepatocytes[12–15] and various adult stem cell sources such as oval cells, small hepatoblasts, hematopoietic stem cells and mesenchymal stem cells.

In this study, we show that 70% of cells derived from mouse ES cells were differentiated into hepatocyte-like cells by coculture with human liver cholangiocyte[16], endothelial[17] and stellate[18] cell lines and growth in fibroblast growth factor (FGF)-2, human activin A and a deleted variant of hepatocyte growth factor (dHGF). ES cell–derived hepatocytes expressed liver-specific genes, secreted albumin and metabolized drugs nearly as well as primary mouse hepatocytes. We also describe a subcutaneously implanted BAL containing ES cell–derived hepatocytes that is easily recharged with additional cells, isolates the hepatocyte cell source from the recipient to reduce the risk of infection and teratoma formation, and does not require connection to the circulatory system, eliminating platelet consumption, hemodynamic instability and the increased risk of bleeding associated with the need for anticoagulants. Use of this device in

[1]Department of Surgery, Okayama University Graduate School of Medicine and Dentistry, 2-5-1 Shikata-cho, Okayama 700-8558, Japan. [2]Roslin Institute, Roslin, Midlothian EH10 4AN, UK. [3]Department of Transplantation, Kyoto University Hospital, 54 Kawara-cho, Shogoin, Sakyo-ku, Kyoto, 606-8507, Japan. [4]Department of Surgery, University of Nebraska Medical Center, Omaha, Nebraska 68198-3285, USA. [5]Institute for Frontier Medical Sciences, Kyoto University, 54 Seigoin-Kawaracho, Sakyoku, Kyoto 606-8507, Japan. [6]Division of Laboratory Products (T.U.), Dainippon Pharmaceutical Co., Ltd., Osaka. [7]Rosalind Franklin Comprehensive Diabetes Center, Chicago Medical School, North Chicago, Illinois 60064, USA. [8]Department of Biochemistry, Chosun University School of Medicine, 375 Seosuk-Dong, Gwangju 501-759, Korea. [9]Geron Corporation, 230 Constitution Drive, Menlo Park, California 94025, USA. Correspondence should be addressed to I.J.F. (ijfox@unmc.edu) or N.K. (immortal@md.okayama-u.ac.jp).

Received 18 August; accepted 6 October; published online 5 November 2006; doi:10.1038/nbt1257